Generating Kolmogorov phase screens for modeling optical turbulence

Alastair D. McAulay[1]

Lehigh University, Bethlehem, Pa 18015.

ABSTRACT

Accurate modeling of turbulence is required for investigating interactions between turbulence, blooming, and environmental and laser beam characteristics. A layered model propagates the optic field across each layer by Fresnel diffraction and a phase screen. Turbulence is modeled statistically with the Kolmogorov spectrum which goes to infinity as spatial frequency decreases. Below a cut-off frequency, the spectrum transitions to zero at a point corresponding to the largest eddies in the turbulence. Two different approaches for computing phase screens with this spectrum are considered. In the first approach, the phase screens are computed directly from the spectrum by inverse transformation. Gaussian random numbers are molded to the spectrum. A discrete 2-D Fourier transform provides sample random phase screens. We show that the discrete Fourier transform cannot provide an accurate transform because of the character of the Kolmogorov spectrum. In the second approach, a covariance matrix is developed using structure functions. This avoids the need to compute a Fourier transform. The eigenvalues and eigenvectors are computed for the matrix. Eigenvalue weighted Gaussian random variables are premultiplied by the eigenvector array to generate phase screens. The advantages, disadvantages, and computational effort are discussed.

1. INTRODUCTION

Accurate modeling of turbulence is important for the design and evaluation of optical communications [13] and optical imaging [16] in the atmosphere, including adaptive optics. Laser beams provide secure optical wireless along the earth's surface and secure satellite communications. For example a number of optical wireless and satellite systems have been successfully constructed and tested with varying communication protocols [9],[14], [4], [2], [10]. Laser weapons are another important application.

Temperature variations in the air over the earth generate convection currents that cause turbulence in the velocity of the air. Turbulence results in eddies of various sizes typically from a few millimeters to an upper bound. In the case of optical wireless along the earth's surface, the largest eddy is approximately 0.4 times the height from the earth's surface [1]. The density variations of the air cause eddies in the refractive index.

Turbulence affects the spatial and temporal properties of the laser beam and interacts with the diffraction process [1],[8],[16],[17]. Spatial spreading of the beam is caused primarily by eddies of size less than the diameter of the beam. Eddies of size greater than the beam diameter act like moving lenses, making the arrive beam wander in the transverse plane in time with an associated time constant. Spatial coherence is degraded, reducing the ability to focus the light. Variations in delay across the beam result in phase interference causing fluctuations in intensity or scintillation. Temporal pulses are spread in time by the temporal characteristics of turbulence and by the varying delay in time resulting from spatial beam wander. In communications, pulse spreading can cause intersymbol interference and reduce signal to noise ratio.

Computing turbulence with the Navier Stokes equation is too computationally demanding although polynomial models have been attempted [12]. Therefore statistical approaches and a layered model of the medium are typically used, figure 1. Light is diffracted between layers. The statistically generated phase screens at each layer represent the phase that would have occurred in propagation through turbulence from the previous layer. The Kolmogorov spatial spectrum is used to generate phase screens for the turbulent medium. The resolution or number of points per unit transverse distance in the cross section aperture is such that the smallest eddies can be accurately modeled. The cross sectional region or aperture is large enough to model the largest eddy size. We assume that the phase screens in different layers are independent.

[1]Email:amcaulay@eecs.lehigh.edu; www.eecs.lehigh.edu/ amcaulay; Phone:610-758-6079; Fax:610-758-6279

In *Laser Weapons Technology*, Todd D. Steiner, Paul H. Merritt, Editors,
Proceedings of SPIE Vol. 4034 (2000) • 0277-786X/00/$15.00

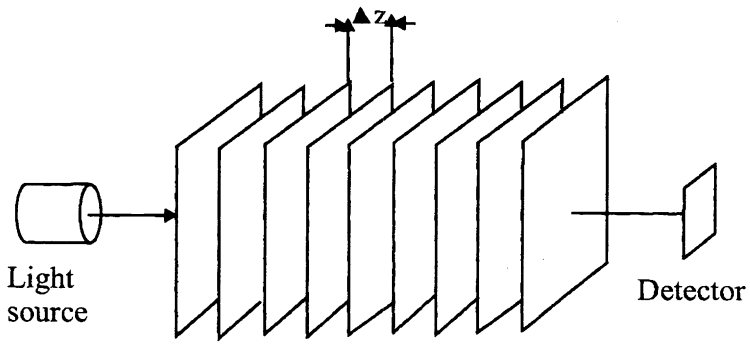

Layered model for turbulence

Figure 1: Sketch showing layered propagation system for modeling propagation of light through turbulent atmosphere.

In section 2 we generate phase screens directly from the Kolmogorov spectrum [5],[11],[3] using the classical fast signal processing approach for generating samples with a specified spectrum. Gaussian random numbers are generated, the square root of the spectrum is impressed on them and a discrete Fourier transform operation performed. A serious problem with this approach is that the Kolmogorov spectrum does not lend itself to taking a Fourier transform because it is not finite unless bounds are applied. If bounds are included there are sharp transitions that cannot be accurately modeled. Therefore some approximations become necessary. In section 3 we consider a much slower method that avoids taking a Fourier transform by computing a covariance matrix directly using a structure function [16]. The method is more versatile because it can include temporal dependencies between phase screens. A method for speeding the algorithm has been proposed [7]. A simulator for testing phase screens is described in section 4.

2. GENERATION OF KOLMOGOROV PHASE SCREENS BY SPECTRAL METHODS

Phase screens are generated directly by Fourier transforming the Kolmogorov spectrum in this section.

2.1. Equations for generating phase screens by FT of spectrum

The Kolmogorov spectral model for turbulence is [1],[16]:

$$\begin{aligned} \Phi(\kappa) &= 0.033 C_n^2 \kappa^{-\frac{11}{3}} \\ &= 0.033 C_n^2 (\kappa_x^2 + \kappa_y^2)^{-11/6} \qquad \text{for } \tfrac{2\pi}{L_0} \le \kappa \le \tfrac{2\pi}{l_0} \end{aligned} \tag{1}$$

where C_n^2 is the strength of the turbulence, κ is the transverse spatial angular frequency for the eddies, L_0 is the maximum eddy size, and l_0 is the minimum eddy size. The spectrum is zero outside of the range of κ specified. Inside the specified range:

$$\Phi(f_x, f_y) = 0.033 C_n^2 (2\pi)^{-11/3} (f_x^2 + f_y^2)^{-11/6} \qquad \text{for } \tfrac{1}{L_0} \le f_x, f_y \le \tfrac{1}{l_0} \tag{2}$$

where f_x and f_y are the spatial frequencies in x and y transverse to the direction of propagation.

For propagation through a layer n of thickness δ_z with light of wavenumber $k = 2\pi/\lambda$ and wavelength λ, the phase changes by:

$$\begin{aligned} (\Phi_n(f_x, f_y))^{1/2} &= (2\pi k^2 \delta_z)^{1/2} \Phi(f_x, f_y) \\ &= 0.09844 (\delta_z C_n^2)^{1/2} \lambda^{-1} (f_x^2 + f_y^2)^{-11/12} \qquad \text{for } \tfrac{1}{L_0} \le f_x, f_y \le \tfrac{1}{l_0} \end{aligned} \tag{3}$$

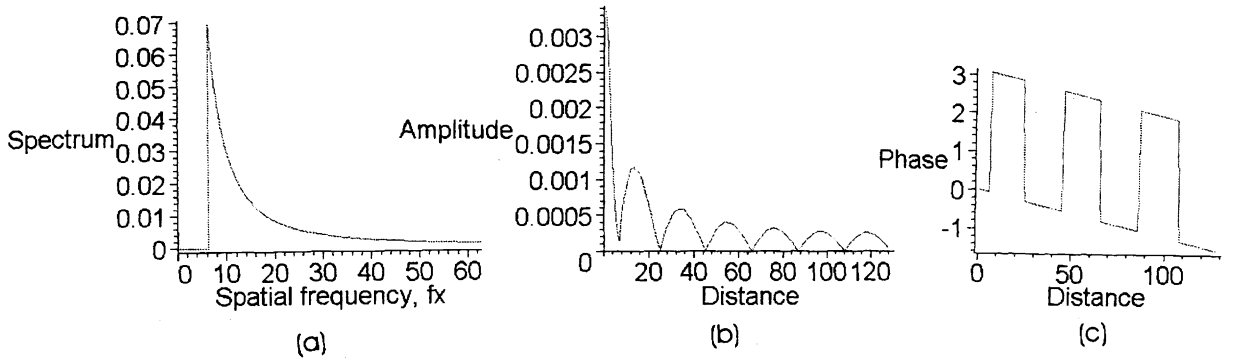

Figure 2: Kolmgorov spectrum in x-direction (a) spatial frequency domain, (b) space domain amplitude from DFT of (a), (c) space domain phase

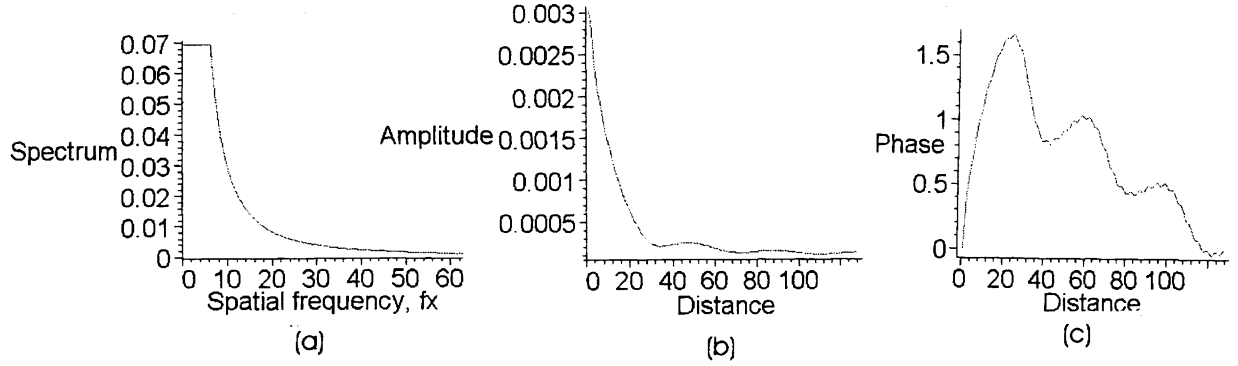

Figure 3: Kolmgorov spectrum in x-direction for constant below lower limit: (a) spatial frequency domain, (b) space domain amplitude from DFT of (a), (c) space domain phase

Figure 2(a) shows a plot of the Kolmogorov spectrum of the phase change across the layer for the x-direction as a function of f_x, equaiotn (3). A smaller eddy represents a higher spatial frequency. Therefore, the decreasing spectral phase magnitude with spatial frequency ($f_x = 2\pi\kappa$) means that there are fewer small eddies than large ones. A difficulty arises because of the need to take a discrete Fourier transform. The sharp transition and the cyclic nature of the discrete Fourier transform result in slowly decaying ringing of amplitude as shown in figure 2(b). The phase is shown in figure 2(c). Note that equation (2) goes to infinity as κ goes to zero in the absence of the limit $2\pi/L_0$. Factoring into two simpler functions before taking the Fourier transform is not helpful as one of the functions will not be finite.

In a preliminary study we assume that the spectrum remains the same below the limit as shown in figure 3(a). Figure 3(b) shows a significant improvement on the rate at which the amplitude falls off. The phase, figure 3(c) is also smoother. The assumption of a non zero dc will cause a change in the average value of the phase screen which will not affect the results significantly. However, we have also added very low frequencies which will produce errors in accuracy of the phase screens. In practice the position of the low frequency cut-off wanders around so that this error is not well defined. The extent and effect of these errors will be determined by comparing phase screens with those generated using the covariance method that avoids taking a Fourier transform (section 3).

Alternatives involving different approximations have been proposed for handling the low frequency cut-off problem for direct transformation from the spectral domain. For example, the Von Karman spectrum [1],[16] gives a smooth function to zero at dc. Similarly polynomials have been used to provide a smooth approximate for the spectrum [5].

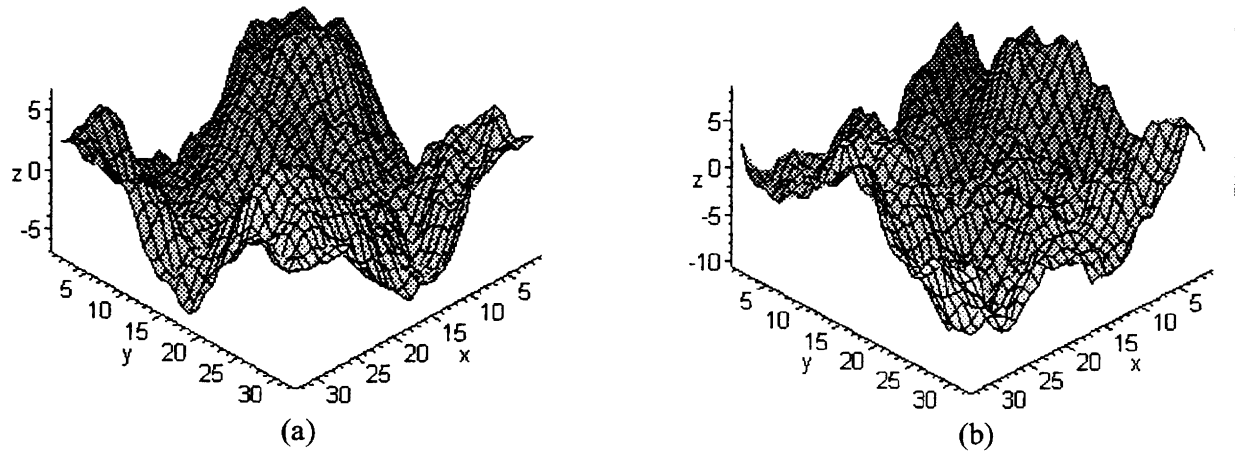

Figure 4: Sample phase screens for Kolmogorov turbulence model: (a) first and (b) second

2.2. Generation and verification of phase screens

Samples of random phase screens with a Kolmogorov spectrum are needed to represent turbulence in the simulator. We follow a conventional approach [3] in which Gaussian white noise is multiplied by the desired spectrum and then the result inverse Fourier transformed. In this case we create two 2-D arrays of Gaussian random numbers for the real and imaginary parts of a complex random variable 2-D array. The complex 2-D array is multiplied by the square root of the Kolmogorov spectrum, equation (3). The sampling of the Kolmogorov spectrum in spatial frequency is selected with an interval of $\Delta f_x = 1/L_0$ so that the first sample is at the lower bound for the Kolmogorov spectrum. This sampling also provides adequate cross section width for the widest anticipated beam. The real and imaginary part of the Fourier transform provide two independent phase screens.

Each call to the phase screen generation function generates a 2-D array of phases for a phase screen. As two phase screens are generated at one time only every second call involves computation, unless the turbulence strength changes between the layers. Four sample phase screens are shown in figure 4(a) and (b) and 5(a) and (b). They vary due to the random model for turbulence. However, they conform to the same Kolmogorov spectral model. Therefore they have the same spatial frequency content. As the Kolmogorov model has less high spatial frequencies the phase screens have a similar spectrally smoothed appearance. A noticeable hill in the phase screen acts as a lens on the light beam. As the hills are off center they will bend the light in a random manner causing the wander of the beam at the receiver. Correct implementation of the equations is verified by averaging the $|FT|^2$ for a 100 random phase screens. The results is identical with figure 2(a).

3. GENERATION OF KOLMOGOROV PHASE SCREENS FROM COVARIANCE USING STRUCTURE FUNCTIONS

The difficulty of taking a Fourier transform of the Kolmogorov spectrum is avoided by working directly with the covariance matrix in the space domain. The approach taken follows reference [16]. A method of speeding up

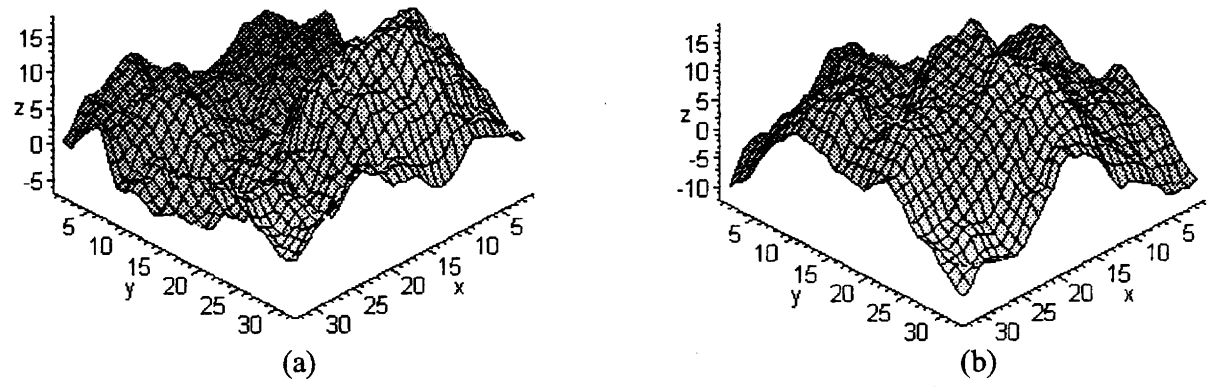

Figure 5: Sample phase screens for Kolmogorov turbulence model: (a) third and (b) fourth

the computation is described in reference [7].

3.1. Equations for computing the phase covariance for the Kolmogorov spectrum

Structure functions are used to construct a covariance matrix from which phase screens are computed. The structure function for a homogeneous (spatially stationary) field f with zero mean is [17]:

$$D_f(r) = E\left[\{f(r_1 + r) - f(r_1)\}^2\right] \tag{4}$$

$D_f(r)$ is large for periodic oscillations with wavelength less that r, providing the structure function with some spectral properties not present in a correlation function. Expanding equation (4) gives:

$$D_f(r) = 2(B_f(0) - B_f(r)) \tag{5}$$

where $B_f(r)$ is the correlation function for f.

The equations for a phase covariance matrix are derived by assuming a phase across a transverse plane and subtracting the mean over the phase screen aperture. The covariance then has four correlation terms. The correlation terms of form $B_f(r)$ are replaced by structure functions $D_f(r)$ from equation (5). The $B_f(0)$ terms cancel. Note that this approach can be readily extended to the case in which phase screens at different layers are dependent [16]. The structure function [15],[8] for the Kolmogorov turbulence model is then used:

$$D_n(r) = C_n^2 r^{2/3} \tag{6}$$

The resulting expression for the phase covariance for one layer is:

$$\gamma_\phi(n, m, n', m') = 6.88 r_0^{-5/3} \left\{ -\frac{1}{2}\left[\{(m - m')\Delta x\}^2 + \{(n - n')\Delta y\}^2\right]^{5/6}\right.$$

$$+\frac{1}{2}\Sigma_{u',v'}^{N_xN_y}\frac{1}{N_x,N_y}\left[\{(u'-m')\Delta x\}^2+\{(v'-n')\Delta y\}^2\right]^{5/6}$$
$$+\frac{1}{2}\Sigma_{u'',v''}^{N_xN_y}\frac{1}{N_x,N_y}\left[\{(m-u'')\Delta x\}^2+\{(n-v'')\Delta y\}^2\right]^{5/6}$$
$$-\frac{1}{2}\Sigma_{u',v'}^{N_xN_y}\Sigma_{u'',v''}^{N_x,N_y}\left(\frac{1}{N_x,N_y}\right)^2\left[\{(u'-u'')\Delta x\}^2+\{(v'-v'')\Delta y\}^2\right]^{5/6}\Bigg\} \quad (7)$$

where the atmospheric coherence length or Fried parameter is:

$$r_0 = q\left[\frac{4\pi^2}{k^2C_n^2\Delta z_i}\right]^{3/5} \quad (8)$$

The atmospheric coherence length r_0 is used to determine the size of aperture at the receiver and the maximum resolution when imaging through turbulence. The parameter q is 0.185 for a plane wave and 3.69 for a spherical wave. The value for the Gaussian beam at the distances of interest are close to that for a plane wave. At $\Delta z = 1000$ m, $r_0 = 0.185$ m which leads to an aperture of approximately 0.2 m square. The propagation constant is $k = 2\pi/\lambda$ and the strength of the turbulence is taken as $C_n^2 = 10^{-13}$. There are many measurements and models for the strength of turbulence [1]. The distance along the propagation path for a layer $\Delta z_i >> N_x\Delta x, N_y\Delta y$. We used $N_x = N_y = 20$ and $\Delta x = \Delta y = 1$ in the simulator.

3.2. Computing a Kolmogorov based phase screen sample for a layer from the covariance

The ingular value decompositon (SVD) computes the eigenvalues, diagonals of Λ, and eigenvectors, columns of U, of the covariance matrix:

$$\mathbf{\Gamma} = \mathbf{U\Lambda U^T} \quad (9)$$

We generate a vector $\mathbf{b'}$ of uncorrelated Gaussian random variables with zero mean and variance Λ of length N_x by N_y. Then:

$$E\left\{\mathbf{b'b'^T}\right\} = \mathbf{\Lambda} \quad (10)$$

where $\mathbf{\Lambda}$ is a matrix with eigenvalues on the diagonal and zero elsewhere. Random phase screens are formed using:

$$\mathbf{a} = \mathbf{Ub'} \quad (11)$$

We verify that the new vector $\mathbf{a}$ has a covariance of Γ by using equations (11) and (10):

$$\begin{aligned} E\left\{\mathbf{aa^T}\right\} &= E\left\{\mathbf{Ub'b'^TU^T}\right\} \\ &= \mathbf{U}E\left\{\mathbf{b'b'^T}\right\}\mathbf{U^T} \\ &= \mathbf{U\Lambda U^T} = \mathbf{\Gamma} \end{aligned} \quad (12)$$

The computation of eigenvalues and eigenvectors is $O(p^2)$ where p is the number of points in an n by n phase screen. This computation of the covariance matrix is no greater than this. One method of speeding up the computation is to precompute eigenvalues and eigenvectors for specific turbulence levels and store these. The generation of phase screens involves only a matrix-vector multiplication which is $O(p^2)$.

4. COMPUTER SIMULATION FOR TESTING PHASE SCREENS

A simulator was constructed to propagate light through turbulent media [13]. The simulator allows comparisons of the effects of different phase screens and comparisons with weak scattering analytical results and with experimental data.

4.1. Description of simulator

A Monte Carlo approach is used in which the diffractive propagation through turbulence is repeated many times on the simulator with different samples of turbulence. The resulting effects are estimated by statistical averaging. The first moment provides the mean beam position, the second the beam spread and the fourth an estimate of the fluctuations in irradiance. The propagation path is divided into layers each having a thickness greatly exceeding the transverse dimensions of the beam, as shown in figure 1. Starting with a Gaussian beam we propagate the beam through each layer. For computational efficiency and convenience we split the computation for propagation through each layer into two steps. In step one we compute the Fresnel propagation [6] through the layer assuming there is no turbulence. In step two we compute the propagation through a sample of a phase screen that approximates the effects of the turbulence on propagation through the layer.

4.2. Propagation through a layer in absence of turbulence

We assume that the distance through a layer, Δz, is much greater than the maximum dimensions transversely in x and y. In this case the Helmholtz wave equations can be approximated by the paraxial wave equation:

$$\frac{1}{r}\left(r\frac{\delta v}{\delta r}\right) + 2ik\frac{\delta v}{\delta z} = 0 \tag{13}$$

Propagation from one plane to another across the layer, width Δz, can be accomplished by using the Huygens-Fresnel principle [6]. This Frensel diffraction can be written as a convolution integral for homogeneous media:

$$U(x,y) = \int\int U(\xi,\eta)h(x-\xi, y-eta)d\xi d\eta \tag{14}$$

where the impulse response is:

$$h(x,y) = \frac{e^{jk\Delta z}}{j\lambda\Delta z} exp\left[\frac{jk}{2\Delta z}\left(x^2+y^2\right)\right] \tag{15}$$

The transfer function is the Fourier transform of the impulse response [6]:

$$H(f_x, f_y) = e^{jk\Delta z} exp\left[-j\pi\lambda\Delta z\left(f_x^2+f_y^2\right)\right] \tag{16}$$

which is an even function of f_x and f_y, allowing computation of one quadrant and replication for the others. Note that convolution in the space domain becomes multiplication in the Fourier transform domain. Therefore propagation of a field U through a distance Δz is achieved by taking its Fourier transform, multiplying by the transform function in equation (16) and then taking the inverse Fourier transform:

$$U(x,y,z+\Delta z) = \mathcal{F}^{-1}\left\{\mathcal{F}U(x,y,z)H(k_x,k_y)\right\} \tag{17}$$

5. CONCLUSION

The effect of turbulence on the propagation of laser light beams was discussed. Methods were described for generating random phase screens to represent the phase change through a turbulent layer. We described the equations and methodology for generating random phase screens directly by discrete Fourier transform of the Kolmogorov spectrum. We showed a plot of the Kolmogorov spectral model for turbulence and explained why there is a problem with accuracy when taking the Fourier transform for generating phase screens because of the low frequency cut off. References to methods to improve the results were provided. Several samples of phase screens were shown with an intuitive explanation of why the beam wanders after propagation through such statistically modeled turbulence. The computation is fast because of the use of 2-D discrete Fourier transforms, taking approximately $O(n^2 log_2 n)$ for an n by n phase screen. A second approach was described that avoids the use of Fourier transforms to provide greater accuracy. The covariance matrix is computed using structure functions and its eigenvalues and eigenvectors are used to generate phase screens. The method is more accurate and flexible, for example it can include dependencies between different phase screens. However, it is more computationally demanding. The generation of the eigenvalues and eigenvectors is $O(n^6)$ (matrix has sides n^2). However if these are precomputed,

only a matrix vector computation of $O(n^4)$ is needed to generate phase screens. We plan to implement a number of different phase screen approaches. The simulator will provide quantitative comparison of the effects of the different choices of phase screens and how well the propagation performance compares with analytical and real data.

6. REFERENCES

1. L. C. Andrews and R. L. Phillips, *Laser beam propagation through random media*, SPIE Optical Engineering Press, Bellingham, Washington, 1998.
2. P. R. Barbier, D. W. Rush, H. Pries, P. Polak-Dingels, and M. L. Plett, "Characterization of optical wireless link performance," SPIE **3532**, pp. 41-8, 1999.
3. G. E. Box and G. Jenkins, *Time-series analysis*, Elsevier, NY, 1976.
4. T. H. Carbonneau, D. R. Wisely, "Opportunities and challenges for optical wireless: the competitive advantage of free space telecommunications links in today's crowded marketplace," SPIE. **3232**. pp 119-128, 1998.
5. W. A. Coles, J. P. Filice, R. G. Frehlich, and M. Yadlowsky, "Simulation of wave propagation in three-dimensional random media," Applied Optics, **34**(12), pp. 2089-2101, 1995.
6. J. W. Goodman, *Introduction to Fourier Optics*, 2nd Edn., McGraw-Hill, New York, 1996.
7. C. M. Harding, R.A. Johnston, and R. G. Lane, "Fast simulation of a Kolmogorov phase screen," Applied Optics, **38**(11), pp. 2161-2170, 1999.
8. A. Ishimaru, *Wave propagation and scattering in random media*, Academic Press, New York, 1978 (or IEEE Press, New Jersey, 1997).
9. I. I. Kim, M. Mitchell, and E. Korevaar,"Measurement of scintillation for free-space laser communication at 785 nm and 1550 nm," SPIE, Optical Wireless Communications II, **3850** Sept. 1999.
10. I. I. Kim, R. Steiger, J. A. Koontz, C. Moursund, M. Barclay, P. Adhikari, J. Schuster, E. Korevaar, R. Ruigrok, C. DeCusatis, " Wireless optical transmission of fast ethernet, FDDI, ATM, and ESCOM protocol data using the TerraLink laser communication system," Optical Engineering, **37**(12), pp. 3143-3155, 1998.
11. J. M. Martin and S. M. Flatte, "Intensity images and statistics from numerical simulation of wave propagation in 3-D random media," Applied Optics, **27**(11), pp. 2111-2126, 1988.
12. A. D. McAulay, "Modeling of deterministic chaotic noise to improve target recognition," **1955**-17, SPIE Signal Processing, Sensor Fusion, and Target Recognition Conference, **1955**-17, April 1993.
13. A. D. McAulay, "Improving bandwidth for line-of-sight optical wireless in turbulent air by using phase conjugation ," SPIE Optical wireless communications II **3850**-5, Sep. 1999
14. G. S. Mecherle and T. Holcombe,"VideoBeam/sup/TM/portable laser communicator," SPIE, **3532**, pp. 22-28, 1999.
15. A. Papoulis, *Systems and Transforms with Applications in Optics*, Robert E. Krieger Publishing Co., Malabar, FL, 1981.
16. M. C. Roggemann and B. Welsh, *Imaging through turbulence*, CRC Press, New York, 1996.
17. , V. I. Tatarski, *Wave propagation in a turbulent medium* McGraw-Hill, New York, 1961.